

A New Solder Paste Inspection Device: Design and Algorithm

Xinyu Wu, Wingkwong Chung, Hang Tong, Jun Cheng and Yangsheng Xu

Abstract—In this paper, we present an innovative design of a solder paste inspection device which can be practically integrated into existing solder paste printing machines. Since solder paste inspection systems usually occupy a large space in vertical direction, we designed a mirror box that can re-direct the transmission of fringe pattern. In this way, a new parallel solder paste inspection device with a significant reduction in the vertical constraint is developed. We also developed a hybrid weighting algorithm that applied the distance and fringe contrast to acquire the height of solder pastes. Furthermore, we developed an algorithm that generates the 2-D image from the fringe pattern images during the 4-Steps Algorithm. It gives benefit (time for solder paste inspection) to traditional approach that uses some special lighting systems to create the 2-D image. Experimental results show our device can inspect the $20\text{mm} \times 20\text{mm}$ PCB area within 2 seconds and the maximum standard deviation for the average height is $3 \mu\text{m}$.

I. INTRODUCTION

NOWADAYS, surface mount technology(SMT) is one of the essential technologies used in electronic industry. A huge of electronic components is packed on small printed circuit boards (PCBs). However, risk of manufacturing problems usually rises when the number of electronics mounted is increased. According to some literatures and manufacturing reports, more than 50% of surface mount PCB manufacturing failures are resulted from solder paste printing processes [1]-[4]. Those failures will lead to the results of reflow and materials wasting. To reduce the manufacturing cost, solder paste inspection is an indispensable process.

Solder paste inspection is mainly non-contact. Many computer vision based 2-D and 3-D solder paste inspection algorithms have been developed in these few years. One of the challenge tasks is to get the height of solder pastes precisely. The most common approach is utilizing the projection of structured light on PCB surface. By analyzing the fringe pattern deformed, height information of solder paste can be obtained.

In general, height acquisition of solder pastes is usually performed by laser-based system [5], [7], [8]. A laser line is first projected on PCB; height of solder pastes is then calculated through triangulation. Because of machine vibration, accuracy of this approach is usually not high. Besides, only one line can be measured in each time of

scanning; the laser system needs to travel to other places for other inspections. Therefore, speed for inspection is also low.

Besides of laser system, phase shifting techniques are also commonly employed. By projecting and analyzing the structured light (fringe pattern), height profile of solder pastes is measured. In 2002, W. C. Lin has applied the projection fringe topography and phase shifting interferometry for 3-D solder paste profile measurement [14]. The algorithm that he applied is 4-Step Algorithm. By the use of phase measuring method, height between a reference plane and PCB surface is determined. However, only using this algorithm can not obtain the height of base board because of the noise. Thereby, we can not obtain the real height of solder pastes. It gives rise to the most challenge task in solder paste inspection. One of the approaches used is the approximation of inspected PCBs by fitting planes. Nevertheless, this approach does not consider the problem of noises in the phase values of base board points.

Furthermore, projection fringe approach is mainly done by the use of a projection lenses system and a camera system (Fig. 1). They are usually arranged in vertical direction (project pattern on PCBs directly). This kind of configuration makes the system occupying a large space, especially in vertical direction. Therefore, the flexibility of this system is low.

In addition, 2-D image used in solder paste inspection is mainly created by the use of another light source. Some of the light sources are light bulbs and LED lights. However, light produced by these devices is usually not even because of the angle of illumination. The control of light source also lowers the speed of inspection. Therefore, an algorithm to create a 2-D image for inspection without 2-D lights is better.

In this project, an innovative solder paste inspection device is developed with the axis of camera parallel to that of projection system. By utilizing a high resolution camera, 4 fringe pattern images are captured. 4-Step Algorithm is then applied to measure the height difference between the PCB's surface and the reference plane. A new approach to generate a 2-D image for the segmentation of solder pastes is also developed. Because of the uneven PCBs' surface, we have also developed a hybrid weighting algorithm to determine the real height of solder pastes on PCBs. To evaluate our inspection system, we have implemented some functions in order to figure out common solder paste defects.

This paper is organized as follows. Section II introduces the parallel solder paste inspection device developed. Section III describes the solder paste inspection of the proposed system. It discusses four major tasks: a) 4-Step Algorithm; b)

The work described in this paper is partially supported by the grant from Sun East Corp., Hong Kong.

X. Wu, W. Chung, H. Tong, J. Cheng and Y. Xu are with the department of Automation and Computer-Aided Engineering, the Chinese University of Hong Kong, Hong Kong, China(email:{xywu, wkchung, htong, jcheng, ysxu}@acae.cuhk.edu.hk).

2-D image synthesis; c) Solder paste height acquisition; and d) 2-D and 3-D solder paste inspection. In Section IV, the performance of the proposed system is evaluated. Experimental results on solder paste inspection are then presented and analyzed. Conclusion and future development are presented in Section V.

II. PARALLEL SOLDER PASTE INSPECTION DEVICE

Many solder paste inspection machines are developed and they are usually isolated from solder paste printing machines. Our goal is to develop a solder paste inspection device that can be integrated into common solder paste printing machines. The most challenge task is to tackle the height constraint caused by traditional inspection systems. A traditional solder paste inspection system using the projection of fringe pattern is shown in Fig. 1. The axis of camera and the axis of projection lenses system are in vertical configuration. This kind of inspection system (including the working distance) is too large to be integrated into a printing machine. To solve this problem, a mirror box is designed and shown in Fig. 2.

In this project, the solder paste inspection device can be divided into two parts. The first one is a high resolution CCD camera (BASLER A202K) used for capturing fringe patterned images. Another part is a projection system. It consists of three components: 1) light source; 2) sine grating; and 3) projection lenses. The inspection area is 20x20mm. The working distance is 48mm from the mirror box to the inspection surface. The camera and projection system are linked together by the mirror box (Fig. 3). Light generated from the light source passes through a sine grating and then a projection lenses. Fringe pattern produced from the projection system will first reach the 30° mirror and then project on the PCB surface. It is reflected from the PCB surface and the 45° mirror. Finally the pattern is captured by the CCD camera (Fig. 4). Through this way, the axis of camera, axis of projection system and PCB are parallel to each other. The working distance is therefore significantly reduced. The sine grating is connected to a micro-positioning system (PI Germany M-110.1). The CCD camera has a resolution of 1004×1003 and the sine grating together with the projection system give 3/mm fringe pattern.

By exploiting our mirror box, direction of light travel is guided and this innovative design gives rise to the integration of this inspection device into solder paste printing machines.

III. FLOW OF SOLDER PASTE INSPECTION

The flow of the solder paste inspection is shown in Fig. 5. PCB for inspection first undergoes the image capturing process with fringe patterns projected on it. Based on the 4 images, we applied the 4-Step Algorithm to obtain the height of solder pastes relative to a reference plane. In parallel, we developed an algorithm to generate a 2-D image used for the segmentation of solder pastes. To get the real height of solder pastes, we implemented a real height acquisition algorithm

based on the application of hybrid weighting. After getting the real height of solder pastes, 2-D and 3-D solder paste inspections are performed.

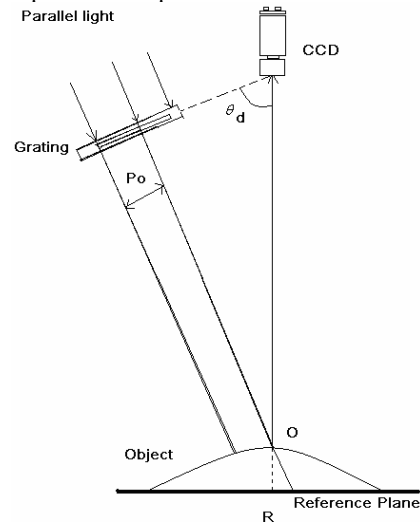


Fig. 1 Solder paste inspection system



Fig. 2 Mirror box

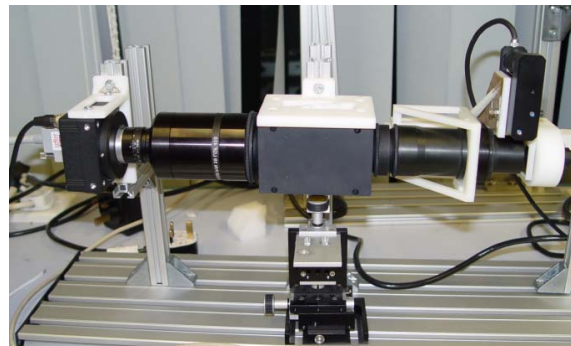


Fig. 3 Parallel design of solder paste inspection device

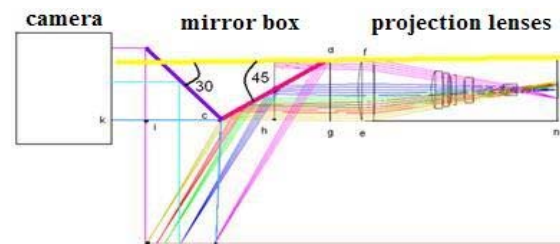


Fig. 4 Optical view of the parallel solder paste inspection device

In this section, we will first introduce the idea of 4-Step Algorithm. Then we will discuss the methodology to create a 2-D image for the segmentation of solder pastes. After that we will discuss a new approach to determine the real height of solder pastes based on the result of 4-Step Algorithm. In the last part, we will talk about the process of 2-D and 3-D solder paste inspection.

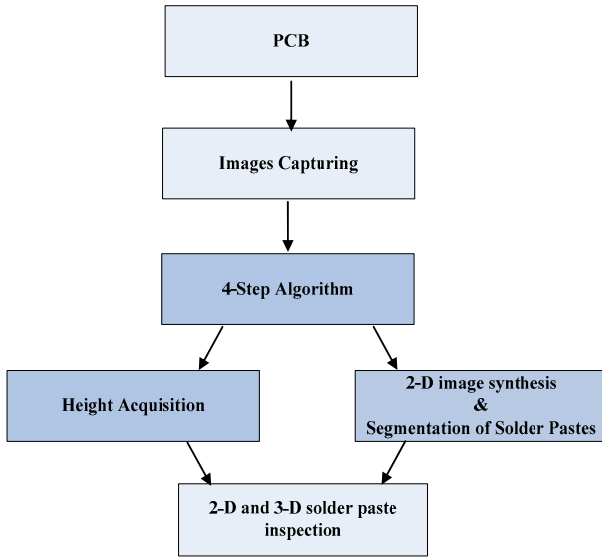


Fig. 5 Flow of solder paste inspection process

A. 4-Step Algorithm

Optical geometry of the parallel solder paste inspection device is shown in Fig. 4. The sine fringe pattern is deformed after projecting on a PCB surface. Through the travel of the micro-positioning system, 4 fringe shift images are captured by the CCD camera. Height profile (h) of the PCB surface relative to a reference plane is calculated by the use of 4-Step Algorithm [10-13].

For every point (x, y) in the inspection region, $h(x, y)$ can be calculated as follows:

$$h(x, y) = \frac{Po}{2\pi} \tan \theta_d \cdot [\phi_r(x, y) - \phi_o(x, y)]$$

$$= \frac{Po}{2\pi} \tan \theta_d \cdot \Delta\phi(x, y) \quad (1)$$

- $h(x, y)$: surface height relative to the reference plane in the image coordinate (x, y)
- Po : the period of the projected fringe of the reference plane
- θ_d : the projection angle of the light ray from the grating
- $\theta_r(x, y)$: phase value in the image coordinate (x, y) of the reference plane image
- $\theta_o(x, y)$: phase value in the image coordinate (x, y) of the object image
- $\Delta\phi(x, y)$: phase difference between $\theta_r(x, y)$ and $\theta_o(x, y)$.

As the term $\frac{Po}{2\pi} \tan \theta_d$ is constant, the equation (1) is simplified into:

$$h(x, y) = k \cdot \Delta\phi(x, y) \quad (2)$$

$$\text{and, } k = \frac{Po}{2\pi} \tan \theta_d$$

The main task in the 4-Step Algorithm is to determine the phase difference $\Delta\phi(x, y)$. During the acquisition, the micro-positioning system travels 4 times per cycle. Therefore, the phase shift of the fringe pattern in each move is $2\pi/4 = \pi/2$. For each fringe shift image, the phase values of both reference plane and object plane can be calculated as follows:

$$\phi(x, y) = \tan^{-1} \left[\frac{I_4(x, y) - I_2(x, y)}{I_1(x, y) - I_3(x, y)} \right] \quad (3)$$

$$I_n(x, y) = I_b(x, y) + I_m(x, y) \cos[\phi(x, y) + (n-1)\frac{\pi}{2}] \quad (4)$$

$n=1, 2, 3, 4$

- I_b is the background intensity
- I_m is the fringe modulation
- $\phi(x, y)$ is the phase at image coordinate (x, y)

As the phase value determined from the equation (3) is in the range $[-\pi/2, \pi/2]$, it is then converted back to $[0, 2\pi]$ (Modulo 2π correction).

$$\phi(x, y) = \begin{cases} \phi(x, y) + 2\pi & \text{if } \phi(x-1, y) - \phi(x, y) > \pi \\ \phi(x, y) & \text{otherwise} \end{cases} \quad (5)$$

B. 2-D Image Synthesis

2-D image is important for the inspection system to make difference between solder pastes and white lines printed on the PCB. Because of the height constraint in solder paste printing machines, it is not possible to integrate an extra LED light into our parallel inspection device. Moreover, the light produced by LED lights is usually not even because of the angle and distance of illumination. Furthermore, 3-D illumination needs time to be stable from 'off' state to 'on' state, the inspection time will be 1.2 seconds longer if both 3-D illumination and 2-D illumination are used. To solve these problems, we create a new algorithm to obtain the 2-D image from the 4 images used by 4-step algorithm.

By solving the equation (4), the background intensity I_b of an image can be computed as:

$$I_b(x, y) = (I_1(x, y) + I_2(x, y) + I_3(x, y) + I_4(x, y)) / 4 \quad (6)$$

Besides, equation (4) can also be expressed in the following form:

$$I_1(x, y) - I_3(x, y) = 2 \times I_m(x, y) \times \cos[\phi(x, y)]$$

$$I_4(x, y) - I_2(x, y) = 2 \times I_m(x, y) \times \sin[\phi(x, y)]$$

Therefore, the fringe modulation I_m can be computed as:

$$I_m(x, y) = \frac{\sqrt{(I_1(x, y) - I_3(x, y))^2 + (I_4(x, y) - I_2(x, y))^2}}{4} \quad (7)$$

Under normal illumination condition, grey value of each pixel in the 2-D image can be expressed as:

$$I_{2D}(x, y) = I_b(x, y) + I_m(x, y) \quad (8)$$

$$\text{with } \cos[\phi(x, y) + (n-1)\frac{\pi}{2}] = 1$$

Results of our algorithm in generating 2-D images are shown in Fig. 6.

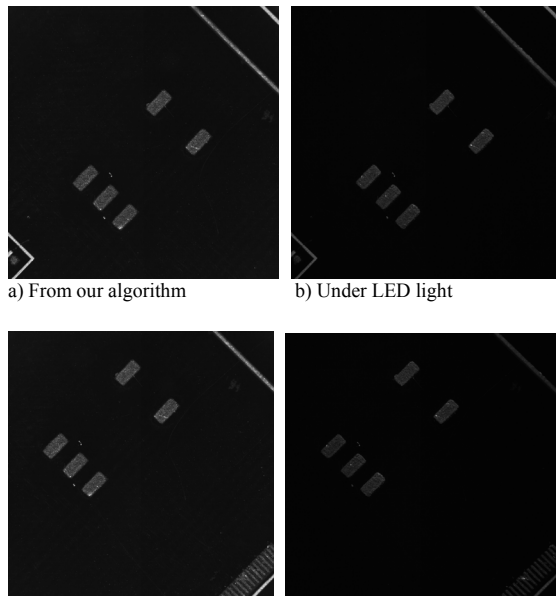


Fig. 6 Results of 2-D images generated by: 1) our algorithm
2) LED light

C. Solder Paste Height Acquisition

From the above equations, phase of each point on PCBs and the reference plane can be determined and the surface height of the inspected PCB relative to the reference plane is then obtained. By calculating the difference between the obtained height values of solder pastes and the PCB base board, height of solder pastes relative to the PCB base board is determined.

Based on the result of 4-Step Algorithm, many approaches have been developed to determine the real height of solder pastes. One of the common approaches is to fit a plane or a series of planes to a PCB surface. Then the real height of solder paste is the height difference between the solder paste and the mean of base board with respect to the reference plane. Another approach is to use the distance from points on base board to the solder paste inspected as a weight. The closer to

the solder paste, the higher the weight assigned. Although height variation of the base board can be minimized by these approaches, noise from the height of base board can not be eliminated. Since the reflectivity of the base board is low, its intensity values in the fringe images are always below 20 (maximal value is 255). If equation (3) is used to compute the phase value of the base board, noise level will be high.

As aforementioned, noise existed in phase values of the base board can not be eliminated by the traditional approaches, a new algorithm is needed. To minimize the influence of the noise, we propose a hybrid weighting algorithm to get the real height of solder pastes. This noise is actually related to the fringe contrast of the 4 fringe pattern images. Therefore, fringe contrast should also be included as a parameter to calculate the weight.

In the hybrid weighting algorithm, a rectangle is first marked on each solder paste (Fig. 7). Size of the rectangle is defined by the area of the solder paste. Since the base board points possess a low reflective index, they can be figured out easily. Then we determine the square of fringe contrast of base board points in the rectangle by the following equation:

$$\gamma(x, y) = \frac{2[(I_4 - I_2)^2 + (I_1 - I_3)^2]}{(I_1 + I_2 + I_3 + I_4)} \times 100\% \quad (9)$$

- I_1, I_2, I_3, I_4 are the intensity values of the same pixel coordinate (x, y) in the 4 images captured during the 4-Step Algorithm

After getting the fringe contrast values, we determine the distances (r) from base board points to their corresponding solder pastes in the rectangle. Then we combine the values of fringe contrast and distance as a hybrid weight (w):

$$w(x, y) = \frac{\gamma(x, y)}{r(x, y)} \quad (10)$$

Weighted average approach is then applied to obtain the real height of solder pastes and is computed as follows:

$$H_i = \frac{\sum w(x, y) \times h(x, y)}{\sum w(x, y)} \quad (11)$$

- H_i is the height of base board inside the i -th rectangle relative to the reference plane
- $w(x, y)$ is the weight assigned to that base board pixel coordinate (x, y)
- $h(x, y)$ is the base board height relative to the reference plane at pixel coordinate (x, y)

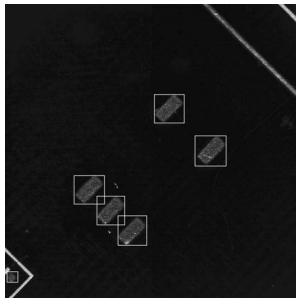


Fig. 7 Idea of weighted average approach

D. 2-D and 3-D Solder Paste Inspection

Based on the results of height acquisition algorithm, 2-D and 3-D solder paste inspections are performed. Firstly, we use a threshold to obtain a binary image from a 2-D image. Then we adopt some morphological operations to remove noises. After the noise removal process, segmentation of solder pastes is performed. A labeled binary image is created. In the labeled image, each solder paste is represented by a unique number.

By mapping the labeled binary image to a standard PCB image, 2-D solder paste defects like solder bridging and solder paste absence can be located. After the mapping process, extraction of solder paste features is performed. They are: a) Area; b) Volume; c) Centroid; and d) Height variation. By utilizing the information obtained, 3-D solder paste defects are located.

IV. SYSTEM PERFORMANCE

In this study, repeatability of the proposed parallel design inspection device is evaluated. The inspection area is defined as $20mm \times 20mm$. A test PCB is first inspected at a particular working distance and orientation. The experiment is then repeated with respect to the variations in two factors: working distance and orientation. The sample PCB is shown in Fig. 8 and the inspection regions are shown in Fig. 9. We test the height acquisition algorithm for many times. Some of the inspection results are shown in Table 1, 2, 3 and 4. For the inspection region shown in Fig. 9a), Table 1 and 2 show the mean value of average height of five solder pastes after 10 experiments (PCB's orientation is varied). When we applied the base board points' distance to a solder paste as weight and compute the real height of solder pastes, maximum standard deviation is $3.3\mu m$. When we applied our hybrid weighting algorithm, maximum standard deviation is $2.8\mu m$ (Table 2).

For the inspection region shown in Fig. 9b), Table 3 and 4 show the mean value of average height of five solder pastes after 10 experiments (working distance is varied). When we applied the distance from base board points to a solder paste as weight, maximum standard deviation is $2.4\mu m$. Our hybrid weighting algorithm shows that the maximum standard deviation is $1.8\mu m$. The overall standard deviation in both experiments is also minimized. Therefore, our hybrid

weighting algorithm can guarantee higher accuracy and system repeatability.

Besides of the above experiments, we have also tested the 3-D performance of the system. Based on the inspection regions shown in Fig. 9b), we changed the PCB's orientation and performed the inspection. The whole process is repeated 15 times(horizontal axis). The experimental results are shown in Fig. 10.

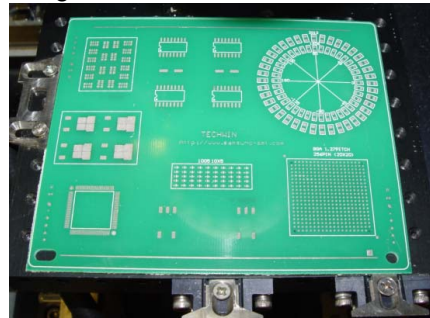


Fig. 8 Testing PCB

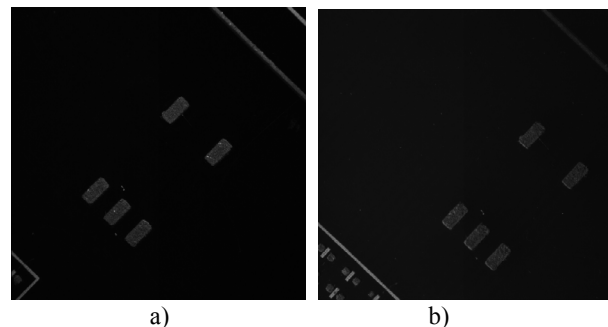


Fig. 9 Inspection regions for the change in a) PCB's orientation b) Working distance

TABLE 1
MEAN AND STANDARD DEVIATION OF THE AVERAGE HEIGHT OF FIVE SOLDER PASTES IN TEN EXPERIMENTS (WITH THE CHANGE IN PCB'S ORIENTATION AND USING DISTANCE TO SOLDER PASTE AS WEIGHT)

Mean (μm)	83.140	89.464	84.693	83.873	86.137
Std (μm)	3.286	2.221	3.259	1.633	2.143

TABLE 2
MEAN AND STANDARD DEVIATION OF THE AVERAGE HEIGHT OF FIVE SOLDER PASTES IN TEN EXPERIMENTS (WITH THE CHANGE IN PCB'S ORIENTATION AND USING HYBRID WEIGHTING ALGORITHM)

Mean (μm)	83.866	91.658	86.141	80.8473	83.030
Std (μm)	2.730	1.569	1.973	1.806	2.048

TABLE 3

MEAN AND STANDARD DEVIATION OF THE AVERAGE HEIGHT OF FIVE SOLDER PASTES IN 10 EXPERIMENTS (WITH THE CHANGE IN WORKING DISTANCE AND USING DISTANCE TO SOLDER PASTE AS WEIGHT)

Mean (μm)	85.719	93.232	89.788	82.799	88.647
Std (μm)	1.290	1.861	1.168	2.350	1.902

TABLE 4

MEAN AND STANDARD DEVIATION OF THE AVERAGE HEIGHT OF FIVE SOLDER PASTES IN 10 EXPERIMENTS (WITH THE CHANGE IN WORKING DISTANCE AND USING HYBRID WEIGHTING ALGORITHM)

Mean (μm)	80.633	87.290	82.857	76.026	80.535
Std (μm)	1.687	0.919	0.880	1.141	1.761

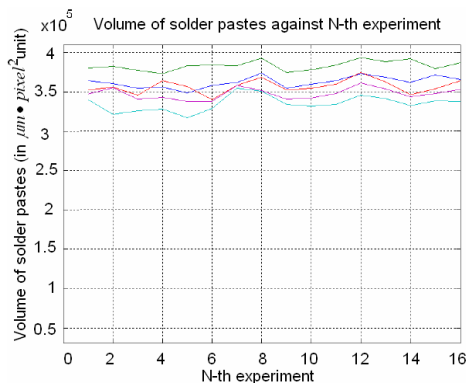


Fig. 10 Variation of volume in 15 experiments(The lines with different color represent different solder pastes)

V. CONCLUSION

In this paper, a fast and complete solder paste inspection device in parallel design has been developed. The target PCB is one with green base board color and the structured light is in sine fringe pattern. Common 2-D and 3-D solder paste defects can be located by this proposed system. Experimental results show our device can inspect the $20\text{mm} \times 20\text{mm}$ PCB area within 2 seconds and the maximum standard deviation for the average height is $3 \mu\text{m}$.

There are totally three contributions in our research: a) An innovative parallel solder paste inspection device using a mirrors box; b) An accurate height acquisition algorithm using a hybrid weighting approach; and c) 2-D image synthesis by the use of inspection images to save inspection time.

In the future, the accuracy of our proposed system can be further improved in the following ways.

- Two separate height acquisition processes can be applied in our system. The idea is to increase the light intensity of the projection system first and the height of the base board relative to a reference plane is measured. Then the intensity is lowered to normal condition and the height of solder pastes relative to the reference plane is measured. It will give higher system accuracy in getting the height of solder pastes than using a single lighting condition.
- Problems like phase discontinuities, low modulation, and regional undersampling of the signal will be considered in the future.

ACKNOWLEDGMENT

The authors would like to thank Weizhong Ye, Zhancheng Wang, Xi Shi and Weimin Li for helping to build the solder paste inspection device presented here. The authors also wish to thank Taikung Au for his assistance on the results.

REFERENCES

- [1] I. Fidan, R. P. Kraft, L. E. Ruff, and S. J. Derby, "Designed experiments to investigate the solder joint quality output of a prototype automated surface mount replacement system," *IEEE Trans. Compon., Packag., Manuf. Technol. C*, vol. 21, no. 3, pp. 172–181, Jul. 1998.
- [2] D. He, N. N. Ekere, and M. A. Currie, "The behavior of solder pastes in stencil printing with vibrating squeegee," *IEEE Trans. Compon., Packag., Manuf. Technol. C*, vol. 21, no. 4, pp. 317–324, Oct. 1998.
- [3] S. C. Richard, "The complete solder paste printing processes," *Surface Mount Technology*, vol. 13, pp. 6–8, 1999.
- [4] J. Pan, G. L. Tonkay, R. H. Storer, R. M. Sallade, and D. J. Leandri, "Critical variables of solder paste stencil printing for micro-BGA and fine pitch QFP," in *Proc. IEEE/CPMT Int. Electron. Manuf. Technol. Symp.*, 1999, pp. 94–101.
- [5] M. Owen, "2-D and 3-D inspections catch solder-paste problems," *Test Meas. World*, vol. 20, pp. 13–18, 2000.
- [6] T. H. Kim, T. H. Cho, Y. S. Moon, and S. H. Park, "An automated visual inspection of solder joints using 2D and 3D features," in *Workshop on Applications of Computer Vision*, 2-4 Dec 1996. Florida.
- [7] T. Okura, M. Kanai, S. Ogata, T. Takei, and H. Takakusagi, "Optimization of solder paste printability with laser inspection technique," in *Proc. IEEE/CPMT Int. Electronics Manufacturing Technology Symp.*, 1997, pp. 361–365.
- [8] Y. K. Ryu and H. S. Cho, "New optical measuring system for solder joint inspection," *Opt. Lasers Eng.*, vol. 26, pp. 487–514, 1997.
- [9] F. C. Yang, C. H. Kuo, J. J. Wing, and C. K. Yang, "Reconstructing the 3D solder paste surface model using image processing and artificial neural network," in *2004 IEEE International Conference on Systems, Man and Cybernetics*, vol.3, no.pp. 3051- 3056 vol.3, 10-13 Oct. 2004.
- [10] V. Srinivasan, H. C. Liu, and M. Halioua, "Automated phase-measuring profilometry of 3-D diffuse objects," *Appl. Opt.*, vol. 23, pp. 3105–3108, 1984.
- [11] S. Toyooka and Y. Iwaasa, "Automatic profilometry of 3-D diffuse objects by spatial phase detection," *Appl. Opt.*, vol. 25, pp. 1630–1633, 1986.
- [12] H. N. Yen, D. M. Tsai and J. Y. Yang, "Full-field 3D measurement of solder pastes using LCD-based phase shifting techniques," *IEEE Transactions on Electronics Packaging Manufacturing*, VOL. 29, NO. 1, pp. 50-57, 2006.
- [13] V. Srinivasan, H. C. Liu, and M. Halioua, "Automated phase-measuring profilometry: A phase mapping approach," *Appl. Opt.*, vol. 24, pp. 185–188, 1985.
- [14] W. C. Lin, "The implementation of a flip chip bump 3D profile online measurement system", Master's Thesis in Chung Yuan Christian University, 2003.